Adaptation of a Bacterial Multidrug Resistance System Revealed by the Structure and Function of AlbA

Asfandyar Sikandar[1], Katarina Cirnski[2,3], Giambattista Testolin[3,4], Carsten Volz[2,3], Mark Brönstrup[3,4], Olga V. Kalinina[5], Rolf Müller[2,3] and Jesko Koehnke[1,*]

[1] Workgroup Structural Biology of Biosynthetic Enzymes, Helmholtz Institute for Pharmaceutical Research Saarland, Helmholtz Centre for Infection Research, Saarland University, Campus Geb. E8.1, 66123 Saarbrücken, Germany

[2] Helmholtz Institute for Pharmaceutical Research Saarland (HIPS), Department of Microbial Natural Products, Helmholtz Centre for Infection Research and Department of Pharmaceutical Biotechnology, Saarland University, Campus E8.1, 66123, Saarbrücken, Germany

[3] German Centre for Infection Research (DZIF), Site Hannover Braunschweig, Braunschweig, Germany.

[4] Department of Chemical Biology, Helmholtz Centre for Infection Research, Braunschweig, Germany. Institute of Systems Biotechnology, Saarland University, Saarbrücken, Germany.

[5] Department for Computational Biology and Applied Algorithmics, Max Planck Institute for Informatics, D-66123 Saarbrücken, Germany

albicidin; cystobactamid; AlbA; antibiotic resistance

ABSTRACT: To combat the rise of antimicrobial resistance, the discovery of new antibiotics is paramount. Albicidin and cystobactamid are related natural product antibiotics with potent activity against Gram-positive and, crucially, Gram-negative pathogens. AlbA has been reported to neutralize albicidin by binding it with nanomolar affinity. To understand this potential resistance mechanism, we determined structures of AlbA and its complex with albicidin. The structures revealed AlbA to be comprised of two domains, each unexpectedly resembling the multi-antibiotic neutralizing protein TipA. Binding of the long albicidin molecule was shared pseudosymmetrically between the two domains. The structure also revealed an unexpected chemical modification of albicidin, which we demonstrate to be promoted by AlbA, and to reduce albicidin potency; we propose a mechanism for this reaction. Overall, our findings suggest that AlbA arose through internal duplication in an ancient TipA-like gene, leading to a new binding scaffold adapted to the sequestration of long-chain antibiotics.

Introduction

Natural products continue to be an abundant source of novel and biologically active molecules (e.g.[1]). The majority of drugs currently on the market to treat bacterial infections are natural products and their derivatives – they have become a major pillar of modern medicine and are regarded as essential for human health[2]. With the extensive use of antibiotics, however, the problem of (multi-)resistance development in human pathogens has risen[3]. To keep pace with resistance development and always have effective antibiotics available, constant antibiotic discovery and optimization efforts are required; a challenge that was not met in the past decades[4]. Most problematic with regard to drug development are Gram-negative pathogens, which are becoming a severe threat to public health[5]. Multidrug resistance (MDR) mechanisms pose a particular challenge, since such systems are able to recognize and neutralize structurally and chemically diverse compounds, while still being selective for a certain compound class[6].

Antibiotic resistance usually results from one of four mechanisms: Modification of the bacterial cell wall to prevent antibiotic entry, expulsion of the antibiotic by general or specific efflux pumps, mutation of the cellular target, or chemical modification of the antibiotic[7-8]. These mechanisms (with the exception of target mutations) are often employed after bacterial antibiotic-specific biosensors bind to an antibiotic and subsequently trigger transcriptional programs[9-10]. One protein class involved in such processes are thiostrepton-induced protein A (TipA) systems[11-12]. TipA belongs to the superfamily of mercuric ion resistance (MerR) -like transcriptional regulators[12-14], which contain an N-terminal helix-turn-helix (HTH) motif, followed by a coiled-coil region and a C-terminal effector binding domain[15-17]. The *tipA* gene contains two alternative start codons, giving rise to TipA-L and TipA-S protein isoforms (Figure 1A)[17-18].

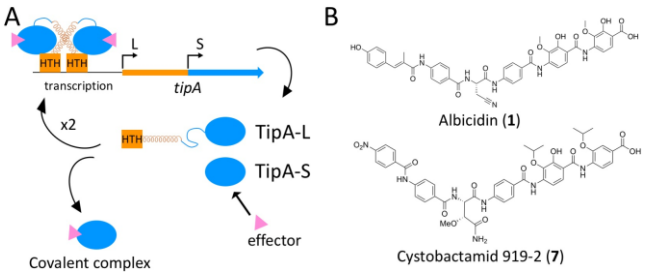

Figure 1 A Basic logic of the TipA system. The *tipA* gene contains two alternative start codons giving rise to TipA-L and TipA-S, which are identical in their C-terminal domains. While TipA-S scrubs free antibiotic from the cytoplasm, TipA-L dimerizes after ligand binding and induces increased expression from the *tipA* gene. **B** Chemical structures of albicidin (**1**) and cystobactamid 919-2 (**7**).

While TipA-L follows the basic MerR architecture, TipA-S is the predominant form and consist only of the effector

binding domain[11-12, 17, 19]. This domain is able to covalently bind a wide variety of thiopeptide antibiotics via an active site cysteine[12, 15-16] and thus permanently sequester the antibiotics[16]. Upon substrate binding, TipA-L forms a dimer, which then binds to promotors via its HTH domain and induces the transcription of multiple genes, including *tipA*, which can thus be viewed as a minimal autoregulated MDR system[11]. Recently reported NMR-based structural studies of TipA-S allowed the proposition of a model for how this protein is able to neutralize a wide variety of thiopeptide antibiotics[15-16]: Upon thiopeptide binding TipA-S transitions from a partially unstructured to a fully ordered state[16]. In the process, a large substrate binding cleft is formed that contains the active-site cysteine, which reacts with the bound substrate to form a covalent bond[16].

The natural products albicidin (**1**) and cystobactamid (**7**) (Figure 1B) were reported as potent anti-Gram-negative antibiotics with minimal inhibitory concentrations (MICs) in the sub-µg/mL range against *Escherichia coli* and other relevant pathogens[20-21]. Albicidin is produced by the plant pathogen *Xanthomonas albilineans*[22-24], and was found to be a strong inhibitor of DNA gyrase in Gram-negative bacteria (*E. coli*)[25]. The unusual structure of albicidin was reported in 2015: It consists of *p*-aminobenzoic acid (PABA) building blocks and cyanoalanine as a central unnatural amino acid (Figure 1B)[26]. Concurrently, cystobactamids, produced by myxobacteria, were discovered as a novel class of antibiotics that address the same bacterial target and possess a similar structure (Figure 1B)[21]. Several differences between the two compound classes exist: While the N-terminus of cystobactamids consists of a *p*-nitro-benzoic acid, the equivalent position in albicidin is occupied by 2-methyl-*p*-coumaric acid. Additionally, the two C-terminal building blocks in cystobactamid 919-2 are isopropoxylated in the 3-position, whereas albicidins are methoxylated, and the C-terminal building block of cystobactamide 919-2 lacks hydroxylation in the 2-position. Finally, the most potent cystobactamids have a central β-methoxy-asparagine amino acid instead of the cyanoalanine found in the original albicidin.

Since antibiotics such as albicidin and cystobactamids occur naturally, resistance mechanisms have already been developed. Three proteins have been reported as resistance proteins against albicidin: AlbA, AlbB and AlbD[18, 27-28]. AlbA is a distant member of the TipA family and can be found in a variety of *Klebsiellae* strains including the problematic human pathogen *K. pneumoniae*. Earlier studies of AlbA reported the protein to bind albicidin at a single high-affinity binding site with low nM affinity and that ligand-binding induced major conformational changes[29-30]. Additionally, an alanine scan of AlbA identified several key residues involved in albicidin binding[29] and it has been suggested that AlbA confers albicidin resistance by removing free albicidin from the cell[18, 31]. During the evaluation of our manuscript, parallel work by Rostock et al. was published[26]. The very thorough biophysical characterization of the AlbA-albicidin interaction using NMR and fluorescence spectroscopy, as well as the crystal structure of the AlbA-albicidin complex were reported. In addition, AlbA was found to protect the albicidin target DNA gyrase from the antibiotic and several derivatives *in vitro* and bacterial cells in an agar diffusion assay[26].

Here, we report the crystal structures of both, AlbA and its complex with albicidin. Unexpectedly, we found AlbA to promote a chemical reaction in albicidin slowly, leading to a loss of biological activity that redefines our understanding of AlbA-mediated albicidin resistance. We provide detailed mutational studies, which allowed us to propose a mechanism for this reaction. We used the structural data to conduct a comprehensive analysis of the prevalence of AlbA-like genes in important human pathogens and their evolutionary development. Finally, we demonstrate that AlbA expression is upregulated in *K. pneumoniae* upon treatment with albicidin.

Results

AlbA is a structural homolog of TipA-S

To understand how AlbA may exert its function, we determined its high-resolution crystal structure. The full-length wild-type AlbA ($AlbA_{wt}$) protein from *K. oxytoca* (see materials and methods for details) formed crystals belonging to space-group $P4_32_12$ and the structure was determined at 1.9 Å resolution by single-wavelength anomalous dispersion using selenomethionine (PDB ID 6h95). All data collection and refinement statistics can be found in table S1. The refined model contained one $AlbA_{wt}$ molecule in the asymmetric unit and includes residues 1 – 221 (Figure 2A). It is an α-helical protein with a flattened, oblong shape measuring approximately 60 Å x 40 Å x 25 Å. $AlbA_{wt}$ has no sequence homologs in the protein data bank (PDB), and we therefore searched for structural homologs using the DALI server[32]. No protein was found to cover more than 50 % of the $AlbA_{wt}$ structure, but upon closer inspection it became apparent that the fully ordered (ligand bound) structure of TipA-S (PDB 2mc0) aligns to the N-terminal 114 residues of $AlbA_{wt}$ (C_α rmsd of 3.7 Å, sequence identity 15 %) and that an additional copy of the same TipA-S structure also aligns to $AlbA_{wt}$ residues 115 – 216 (C_α rmsd of 3.9 Å, sequence identity 16 %) (Figure 2B and S1). Following TipA-S nomenclature[15-16] (TipA-S consists of helices α6 - α13), $AlbA_{wt}$ does not contain α6, but all other helices are largely conserved. Helices α7 and α8, which are critical for substrate binding in TipA-S[15-16], are much shorter in $AlbA_{wt}$ and do not form the deep substrate binding cleft observed in TipA-S[15-16]. Best conservation (helix length and relative position) is observed for α9 and α10. Intriguingly, unlike TipA-S, α11 and α13 of $AlbA_{wt}$ are neither parallel nor in direct contact with each other, but spread apart (Figure 2C). In $AlbA_{wt}$, helix α13 is significantly longer than in TipA-S and its C-terminal portion aligns with α7 of the second TipA-S copy (TipA-S') (Figure 2B and S1). The alignment of TipA-S' α8 - α13 with $AlbA_{wt}$ α8' to α13' corresponds to the alignment of TipA-S with the N-terminal half of $AlbA_{wt}$. It thus appears that AlbA originated from an internal gene duplication event in a TipA-S-like gene, giving rise to a pseudosymmetric TipA-S dimer. In addition to the change in binding-site architecture, the residues identified as important for substrate binding, including the active-site cysteine, show no conservation. In TipA, the cysteine reacts with dehydroalanine residues when TipA-S/L bind thiopeptide antibiotics to form covalent complexes[12, 33], chemistry which would not be possible with albicidin. Binding of albicidin must therefore follow a different logic, and we identified a putative substrate binding tunnel, which runs across the entire length of the

protein (Figure S2). Its formation is a direct result of the movements of helices α11 / α13 and α11' / α13' (Figure S3).

Structure of the AlbA$_{wt}$ -albicidin complex

In order to understand how albicidin may fit into the putative substrate binding tunnel of AlbA we determined the high-resolution structure of the AlbA$_{wt}$-albicidin complex. The natural product albicidin was synthesized according to a previously published procedure (see supplementary online material)[20].

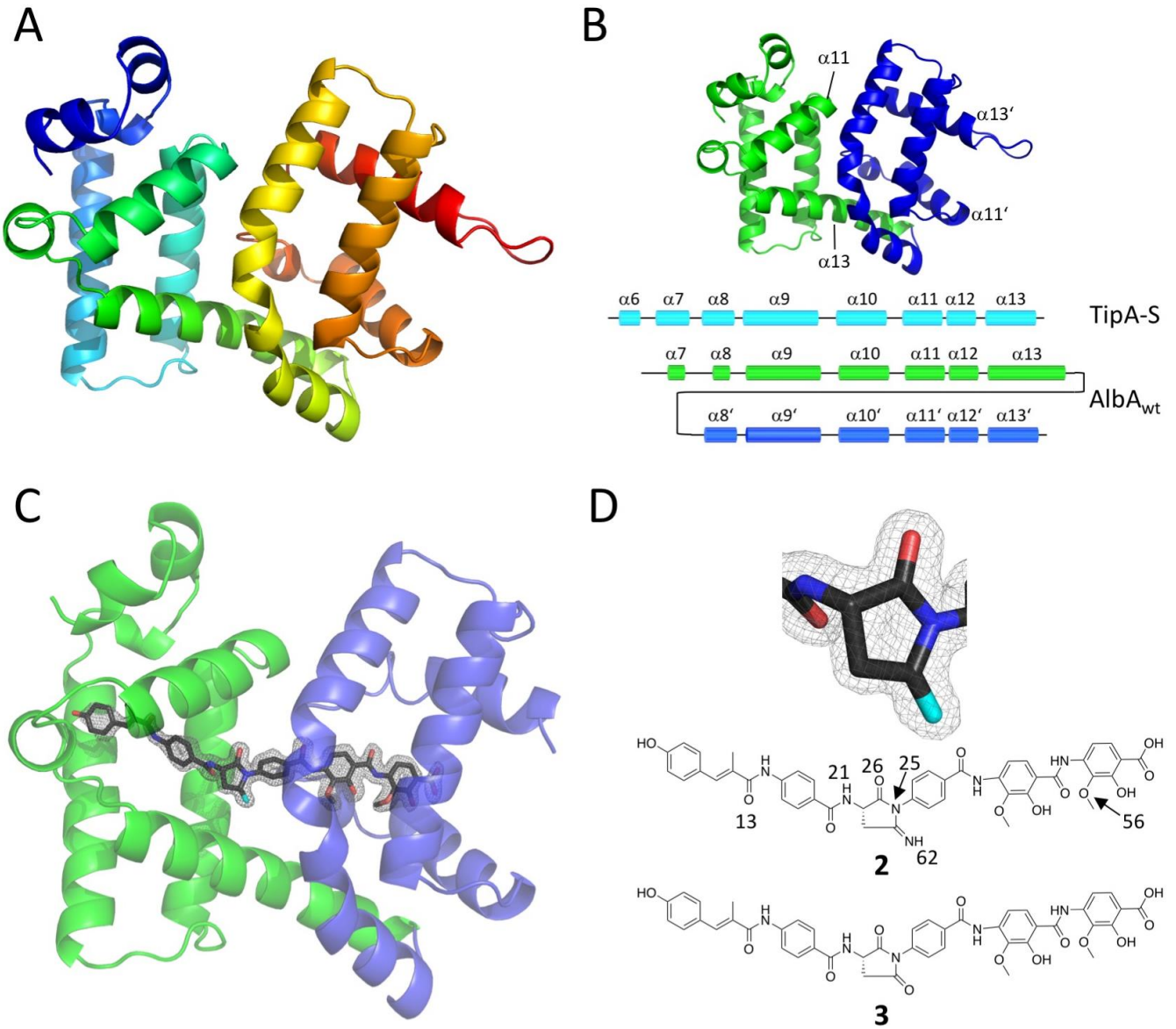

Figure 2 A Overall structure of AlbA$_{wt}$. The structure of AlbA$_{wt}$ is shown in cartoon representation using the rainbow color scheme (N-terminus blue, C-terminus red). **B** AlbA is a tandem repeat of TipA-S. The AlbA$_{wt}$ structure is shown as a cartoon representation with the N-terminal TipA-S repeat in green, and the C-terminal TipA-S repeat in blue. Helices that underwent a drastic change in orientation and relative position in AlbA$_{wt}$ (when compared to TipA-S) are labeled. A secondary structure diagram shows the conservation of helix length and position between the two proteins. **C** AlbA$_{wt}$-albicidin complex structure. Protein representation and color scheme as in B. Albicidin is represented as sticks. Carbon atoms black, oxygen atoms red, nitrogen atoms blue, unassigned atom cyan. The difference electron density (*F*o – *F*c contoured at 3σ with phases calculated from a model which was refined with no albicidin present) is shown as a grey isomesh. **D** Chemical structures of the two possible albicidin conversion products, the primary ketimine **2** and the succinimide **3**.

AlbA$_{wt}$ was incubated with an excess of albicidin and subsequently crystallized in space group C222$_1$. The structure was determined to 1.55 Å resolution by molecular replacement using the structure of AlbA$_{wt}$ as a search model (PDB ID 6h96).

The new crystal form contained two AlbA$_{wt}$ monomers in the asymmetric unit and the overall structure of AlbA$_{wt}$ is virtually unchanged after binding albicidin (Rmsd of 0.8 Å over all non-hydrogen atoms, Figure S4). It has been reported that the NMR spectra of AlbA show extensive line-broadening in the absence of albicidin, which may be caused by slow internal dynamics of the protein[26]. This observation led to the hypothesis that AlbA may exist in an open and closed conformation, with an ensemble of intermediate

states[26]. Since the AlbA structure we determined corresponds to the AlbA-albicidin complex structure, we suggest that we have crystallized the closed conformation of the protein. We observed clear and unambiguous electron density for albicidin, spanning the entire length of AlbA (Figure 2A and S5), with binding of the extended albicidin molecule shared pseudosymmetrically between the two TipA-S domains. Upon closer inspection of the electron density for the ligand, it became obvious that the central cyanoalanine moiety had cyclized to yield a five-membered ring, in which the nitrile group had been converted to a primary ketimine or succinimide (**2** and **3**, respectively, Figures 2D and S5). Equivalent electron density was also reported by Rostock et al. (PDB ID 6et8)[26], but an unmodified albicidin molecule was built into the density, which resulted in a poor fit, high B-factor of the nitrile carbon compared to adjacent atoms and very close interatomic distance between the amide proton of NH25 (numbering in Figure 2D) and the triple bond of the nitrile moiety (1.4 Å) (Figure S5). Albicidin is almost completely buried in the AlbA tunnel and engages in extensive hydrophobic interactions. A complete LigPlot interaction diagram can be found in Figure S6. Several residues identified previously as important for albicidin binding through an alanine scan[29] are in fact in contact with albicidin. In addition to the hydrophobic interactions, AlbA and albicidin form a salt-bridge and several hydrogen bonds, all mediated by side-chains. The carbonyl oxygen O13 (numbering in Figure 2D) forms a hydrogen bond with H78, while N75 is a bidentate ligand, forming hydrogen bonds with NH21 (immediately adjacent to the five-membered ring) and O26 (part of the newly formed ring). The ketimine / ketone moiety (NH / O62) is hydrogen bonded to T99, and the final interactions concern the terminal *para*-aminobenzoic acid unit. The side-chain of Y169 is hydrogen-bonded to O56 (methylated *m*-oxygen), while Q205 and R181 form a hydrogen bond and salt bridge, respectively, with the terminal carboxyl group. These extensive interactions explain the high affinity of $AlbA_{wt}$ for albicidin.

$AlbA_{wt}$ promotes the cyclization of albicidin

We wondered whether the observed five-membered ring was an artefact or an AlbA-mediated modification of albicidin. When equimolar amounts of $AlbA_{wt}$ and albicidin (100 µM each) were incubated at 37 °C for 24 h prior to analysis by high-resolution liquid chromatography-mass spectrometry (HR-LCMS), we discovered that the $AlbA_{wt}$-albicidin sample contained four additional peaks (Figure 3A). In contrast, control samples set up in the reaction buffer with BSA (Figure S7) or without protein (Figure 3A) showed no conversion of albicidin. In fact, only traces of converted albicidin could be detected in reaction buffer without protein after 14 days at 37 °C (Figure S7). This reaction was temperature-dependent – after 24 h, no conversion was observed at 4 °C, while little conversion was detected at 20 °C. At 37 °C, more than half of the albicidin was converted (Figures 3A and S8).

In the $AlbA_{wt}$-containing sample, the peak representing albicidin (m/z calc: 843.2620, observed: 843.2621, Δppm 0.1) had decreased significantly, while two new main peaks appeared. The most abundant species was an isotopomer of albicidin with a different retention time, indicating **2** (m/z calc: 843.2620, observed: 843.2632, Δppm 1.4), which was supported by tandem mass spectrometry (MS^2, Figure S9). Since primary ketimines are unstable in aqueous solution, we expected the third main peak to be the hydrolysis product of **2**, the succinimide **3** (m/z calc: 844.2461, observed: 844.2466, Δppm 0.6), and the identity of **3** was in agreement with MS^2 data (Figure S10). The two minor peaks had near identical masses, and we assigned them as two diastereomers of the intermediate between **2** and **3**, corresponding to a hemiaminal **4** (m/z calc: 861.2726, observed: **4a** 861.2740, Δppm 1.6 and **4b** 861.2738, Δppm 1.4). While it is not possible to determine which peak corresponds to which diastereomer, MS^2 data corroborated the assigned identity of the compounds (Figures S11 and S12). To ascertain whether **2** or **3** was found in the $AlbA_{wt}$-albicidin complex structure, we harvested multiple AlbA-albicidin crystals, washed them thoroughly and dissolved them in acetonitrile prior to MS analysis. The predominant species was **2**, with a small fraction of **3** that is likely the result of hydrolysis during analysis of the sample and traces of **1** (Figure S8). Therefore, rather than just neutralizing albicidin by binding to it, $AlbA_{wt}$ fosters the conversion of albicidin to **3**, with **2** representing the protein-bound (and solvent-protected) intermediate.

To better understand the albicidin conversion, we set up a time course experiment and observed a nearly completed process after 64 h when using a 1 : 1 molar ratio of protein and compound (Figure S13). This very slow progression would imply that despite the non-covalent nature of their interaction, cells would still have to produce stoichiometric quantities of $AlbA_{wt}$ for protection, mirroring the situation for TipA. When sub-stoichiometric quantities of $AlbA_{wt}$ were used, the conversion progressed very slowly, but one $AlbA_{wt}$ molecule was able to promote cyclization of multiple albicidin molecules (Figure S13).

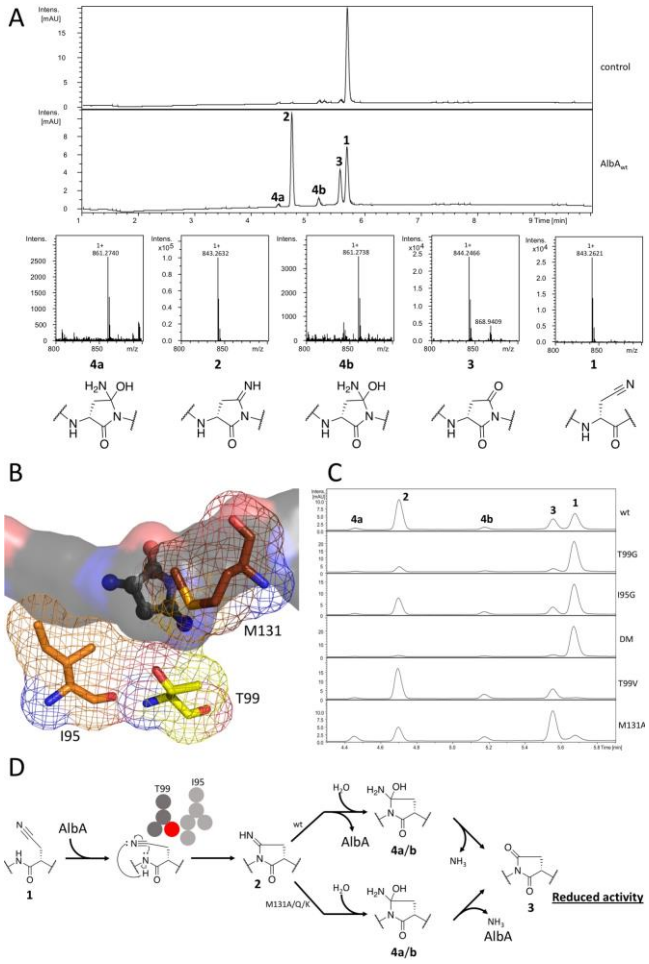

Figure 3 A Incubation of albicidin with AlbA$_{wt}$ leads to the cyclization of albicidin at the cyanoalanine moiety. The four product peaks were assigned to their chemical structures by MS^2 (see SOI). **B** Three residues are in direct contact with the newly formed ketimine: I95 (orange), T99 (yellow) and M131 (brown). Their surface is represented as an isomesh with corresponding colors. The solid surface of albicidin is colored as carbon atoms black, nitrogen atoms blue, oxygen atoms red. The ketimine moiety is shown as a ball and stick model using the same color scheme. **C** The effects of four point- and one double-mutant (DM, I95G/T99G) on albicidin. The **3** : **2** ratio is inverted for AlbA^{M131A} when compared to the other mutants or wt protein. **D** Proposed mechanism for albicidin conversion. While the **2** has to be released from the protein before it can hydrolyze to **3**, mutation of M131 to Ala or a hydrophilic residue allows hydrolyzation while **2** is still bound to the protein.

Interestingly, we also detected varying amounts of the hydrolysis product of **3** in samples containing substoichiometric AlbA concentrations, in which the central linker is either an aspartate or iso-aspartate (m/z calc: 862.2566, observed: **6** 862.2569, Δppm 0.3, Figure S13). Formation of **6** is possibly the result of the extensive incubation time required and this variant of albicidin has been reported to be inactive[34]. We speculated that the relative affinities of **1** and **2** may be a reason for slow cyclization. When we analyzed the interaction of AlbA$_{wt}$ with albicidin by surface plasmon resonance (SPR), the K_D for this interaction was calculated as 2.1 nM (Figure S14), which is on par with the K_D reported by Rostock et al.[26]. The main contributor to this high affinity was the very slow off-rate of just 1.1 x 10^{-4} s^{-1}, which may explain the slow progression of cyclization observed at substoichiometric protein concentrations.

The affinity of **3** was slightly weaker (11.6 nM) and, crucially, **3** retained a very slow albeit slightly faster off-rate of 2.8 x 10^{-4} s^{-1} (Figure S14). This implies very slow release of **2**/**3** may be the main contributor the slow progression of cyclization. Overall these data therefore argue that AlbA, in addition to being a very strong albicidin binder, aids in the cyclization of albicidin. We are unaware of comparable processes in natural products.

Rationalizing AlbA activity

We expected cyclization of albicidin to **2** to follow standard chemistry – deprotonation of the amide nitrogen (NH25), followed by nucleophilic attack on the nitrile carbon and subsequent protonation of the intermediate to yield the primary ketimine function. Since the amide nitrogen would be a weak nucleophile, we suspected that the reaction may be aided by protonation of the nitrile nitrogen prior to nucleophilic attack, but no aspartate or glutamate residues were found in close proximity. To shed light on the reaction mechanism, we first investigated the effects of general acid and / or base. We incubated AlbA$_{wt}$ with an equimolar amount of albicidin at different pH values from 5.5 to 9.0 in increments of 0.5 (Figure S15). At low pH, we observed little cyclization, but as the pH increased, so did cyclization. No cyclization was observed in control reactions without AlbA$_{wt}$ unless Tris buffer was used, in which case we observed slow, AlbA$_{wt}$-independent cyclization of albicidin at pH 8.5 and 9.0 (Figure S15). While a normal peptide amide would not be deprotonated under such mild conditions, the amide in question can be viewed as an aniline-derivative with a carbonyl group in the *p*-position, which presumably significantly lowers the pK_a of this amide. These observations are suggestive of the involvement of a general base.

A detailed analysis of the residues in direct contact with the newly formed ketimine – I95, T99 and M131 – was performed (Figure 3B). The side-chain of T99 packs against the side-chain of I95 and is hydrogen-bonded to the ketimine. We thus wondered whether T99 played a role in cyclization and produced AlbA^{T99V} and AlbA^{T99G}. All mutants reported expressed like wild-type protein and showed highly similar elution profiles in size-exclusion chromatography (Figure S16). The overall structure of apo-AlbA^{T99V} (PDB ID 6h97), determined at 2.7 Å resolution (Table S1), was unchanged and the mutant side-chain had the same orientation and position as T99 in the AlbA$_{wt}$ structure (Figure S17). When we tested the effect of AlbA^{T99V} on **1**, we found cyclization to be accelerated ~2.5 x when compared to the wt protein (Figures 3C and S18). In contrast, AlbA^{T99G} promoted little cyclization, even after 24 h (Figure 3C). We thus propose that the side-chain of T99 creates a bottleneck in the albicidin binding tunnel, that forces the nitrile group of albicidin into a position that favors nucleophilic attack of amide N25 on nitrile C28, leading to the formation of **2** (Figure 3D). By exchanging the threonine to a slightly bulkier valine, we strengthened the hydrophobic interactions between I95 and the amino acid in position 99 (now V). This could lead to a more stable barrier and thus promote faster cyclization of albicidin. Accordingly, with the barrier largely removed in AlbA^{T99G}, albicidin cyclization was almost abolished. In

agreement with this hypothesis, AlbA^{I95G} showed reduced but still appreciable effects on albicidin (Figure 3C), since now merely the back-stop of the actual barrier was removed. When incubated with the double mutant, AlbA$^{I95G/T99G}$, albicidin was virtually unaffected (Figure 3C).

The position of the side-chain of M131 appeared to protect the ketimine function of **2** from bulk solvent and to prevent the formation of the hemiaminal **4**a/b during hydrolysis of **2**. In consequence, one would expect a mutation of the methionine to a residue with a less bulky side-chain to promote the formation of **3**. Accordingly, AlbA^{M131A} incubated with albicidin, led to a much larger percentage of **3** than the wt protein or any previously analyzed mutant (Figure 3C). We determined the complex structure of AlbA^{M131A} with albicidin at 2.2 Å (PDB ID 6hai) (Figure S19 and Table S1). In the structure, the small alanine side-chain affords ample room to form the hemiaminal intermediate (Figure S20). It should be noted that in the complex structure of AlbA$_{wt}$ with **2**, two ordered water molecules (HOH6 and 102) are in a position to attack the ketimine carbon (Figure S20) and may promote hydrolysis.

Cyclization decreases albicidin activity, but AlbA is insufficient to protect cells from albicidin

An important question with respect to the resistance mechanism exerted by AlbA was whether the protein-mediated modification altered albicidin activity. We attempted to purify **2** and **3** in sufficient quantities for biological testing by setting up large-scale conversion reactions. As expected, it was not possible to purify **2**, as the peak converted to **3** during purification. Compound **3**, on the other hand, was stable and we tested its activity against *E. coli*, *Staphylococcus aureus*, *Bacillus subtilis* and *Micrococcus luteus* (Table 1). The most pronounced effects were observed for *E. coli* and *S. aureus*, where **3** showed a decrease of activity by 300 x and 222 x, respectively. For the other two strains, activity was reduced by approximately two orders of magnitude. We have therefore been able to demonstrate that the modification of albicidin to **3** results in a significant decrease of albicidin activity.

Table 1: Activity of 3 and 1 on selected bacterial strains. Cyclization of cyanoalanine to succinimide leads to a significant decrease in activity.

		E.coli DSM1116	*S. aureus* Newman	*B. subtilis* DSM10	*M. luteus* DSM1790
MIC (µg/mL)	**3**	1.8	28.8	5.4	43.5
	1	0.006	0.13	0.03	0.5
MIC shift	**3/1**	300	222	108	87

A

	E. coli BL21 (DE3)	+ $AlbA_{wt}$	+ $AlbA^{M131Q}$	+ $AlbA^{M131K}$
1	< 0.03	< 0.03	< 0.03	> 64
7	< 0.03	< 0.03	< 0.03	16

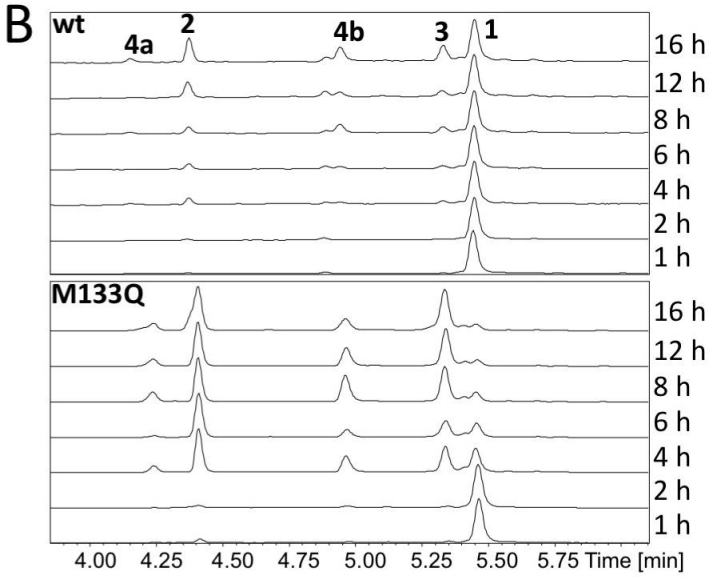

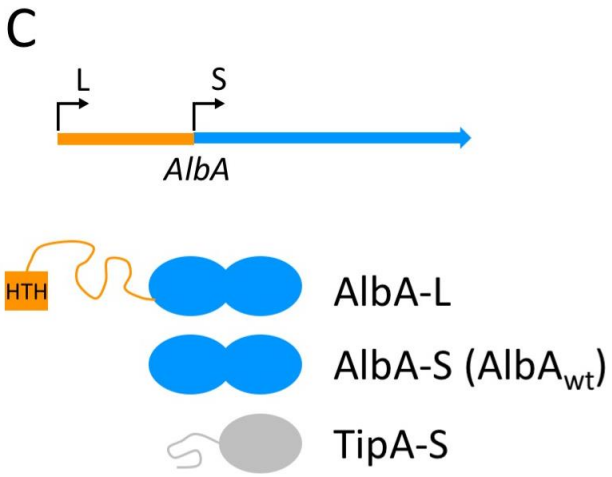

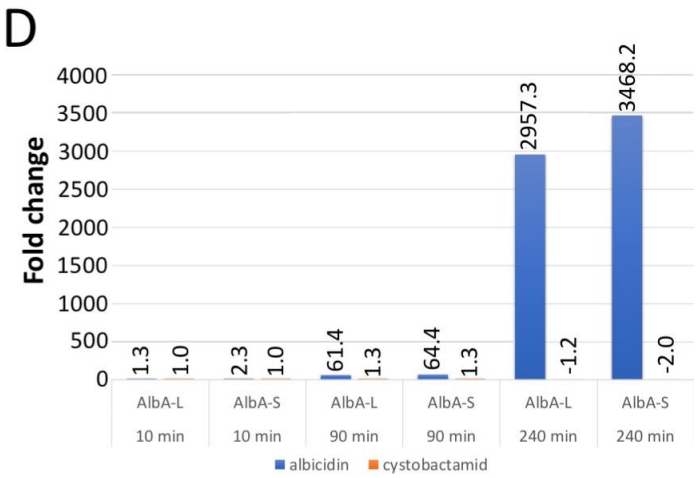

Figure 4 A MICs demonstrating that $AlbA_{wt}$ is insufficient to protect *E.coli* BL21 (DE3) from **1** or **7**. Naturally occurring point-mutation M131K on the other hand renders these cells albicidin resistant and protects the cells largely from **7**. MICs are given as compound concentrations (μg/mL) **B** Time-course for the cyclization of albicidin when incubated with $AlbA_{wt}$ (top) and $AlbA^{M133Q}$ (bottom) using 1 : 1 protein : compound ratios. The M131Q point mutation leads to significantly accelerated cyclization. **C** Reevaluation of the *albA* sequence reveals an alternative start codon upstream of the reported start. Translation from the alternative start codon would yield an AlbA-L protein that also contains an N-terminal HTH motif followed by a random coil, analogous to TipA. **D** RT-qPCR results demonstrating that exposure of *K. pneumoniae* to **1**, but not **7** induces *albA* transcription.

It has been demonstrated in agar diffusion assays that when AlbA is pre-incubated with an equimolar amount of albicidin, the remaining concentration of free albicidin is too small to inhibit bacterial growth[26]. The same observation was made for the activity of DNA gyrase, the albicidin target, *in vitro*[26]. Since the read-out of these experiments is compound-protein affinity, we wondered if *E.coli* overexpressing AlbA would be resistant to albicidin. When we tested *E.coli* BL21 over-expressing AlbA, we found the cells to be susceptible to **1** (Figure 4A). Since *Klebsiellae* containing the *albA* gene are fully resistant to albicidin[20-21], it thus appears highly probable that additional factors are required for albicidin resistance.

Evolution of AlbA and evidence for a more efficient homolog in *K. pneumoniae*

We aimed to understand how AlbA-mediated albicidin resistance had evolved and how widely proteins that could potentially bind albicidin and related compounds are distributed amongst sequenced proteobacteria. A search of the non-redundant database for AlbA homologs returned 1,906 sequences from beta-, gamma-, and delta-proteobacteria, all of which were annotated as mercuric ion resistance (MerR) family transcription regulators. Next, we used the AlbA-albicidin complex structure to define the residues in direct contact with albicidin and how each of these residues could be varied to still allow albicidin binding. This contact pattern (Figure S21) was then used to filter the obtained homologs. Phylogenetic analysis reveals that this pattern can occasionally be found in *Klebsiella* and *Enterobacter* species, as well as in several closely related sequences from *Raoultella*, *Kosakonia*, *Kluyvera*, *Escherichia*, *Pseudoescherichia*, and *Leclercia* spp.. The distribution of the relevant sequences in the phylogenetic tree (Figure S22) suggests that in *Klebsiella* and *Enterobacter* the pattern evolved on several independent occasions, whereas in *Rauoltella*, *Kosakonia*, *Kluyvera*, *Escherichia*, *Pseudoescherichia*, and *Leclercia*, close homology coupled with the virtual omnipresence

of sequences containing the contact pattern suggests introduction of the protein into these species via horizontal gene transfer as a means of resistance against albicidin. Additionally, the *Raoultella* branch is embedded into the *Klebsiella* branch, which suggests *Klebsiella* as the source of the horizontal gene transfer into *Raoultella*. For other species, the phylogeny is not well resolved at the branching point, so the source of the transfer is more difficult to pinpoint.

Since AlbA was originally discovered in *K. oxytoca*, we had a closer look at the evolution of AlbA in *Klebsiellae* as a whole. When searching for AlbA homologs in publicly available whole genome sequencing data and filtering identical sequences, two clades of AlbA were found: One group, consisting mostly of *K. oxytoca* and *K. michiganensis* strains, is currently comprised of 36 sequences with no less than 90 % homology to AlbA. These sequences contain no variations in the residues making contact with albicidin. The second group contains 129 sequences that are all 77 ± 2 % identical to AlbA and is found mainly in *K. pneumoniae*, *K. variicola*, and *K. quasipneumoniae*. These sequences contain a single point mutation in the residues contacting albicidin. Here, the M131 residue, which has been identified by us as critical to shield the intermediate **2** from water, is mutated to either Q (most cases) or K (some instances). The exchange of M131 to a hydrophilic residue opened the possibility that these AlbA homologs would behave in a manner similar to AlbA^{M131A}. We therefore introduced the point mutations M131Q and M131K into AlbA$_{wt}$ and analyzed the effects of these mutations on albicidin cyclization. Both mutants promoted much faster cyclization of albicidin than the wild-type protein (Figure 4B), with the lysin mutant being faster than the glutamine mutant. When the more prevalent mutant M131Q was used at sub-stoichiometric concentrations it showed faster cyclization than AlbA$_{wt}$ (Figure S23). Interestingly, we did not observe the same effect of pH on AlbA^{M131Q} as AlbA$_{wt}$, which may suggest that the glutamine now acts as a specific base to promote the reaction (Figure S23). We were curious whether these mutations altered the behavior of AlbA enough to now allow AlbA to protect cells from albicidin. When we tested *E.coli* over-expressing AlbA^{M131Q} or AlbA^{M131K}, we found the M131Q mutation to have no effect on the minimum inhibitory concentration (MIC) of albicidin. In stark contrast, cells overexpressing the M131K mutant were fully resistant to albicidin (Figure 4A). Whether this is a direct function of cyclization or involves additional factors will require further study. It thus appears as if a version of AlbA that is more efficient at protecting cells from albicidin already preexists in the microbial community and may be passed on to critical human pathogens via horizontal gene transfer. In fact, several instances of this point mutation can be found in AlbA homologs present in *E. coli*.

AlbA defines a new TipA-like family

One characteristic of the AlbA homologs from both clades described above was prominent: Virtually all possess an N-terminal extension when compared to AlbA. This extension has homology to known HTH DNA-binding domains of transcription factors and is followed by a coiled-coil region, after which homology to AlbA begins. The basic architecture of these AlbA homologs therefore resembles that of the autoregulatory TipA system, with a substrate binding domain that has been extended through internal gene duplication. A closer look at AlbA reveals the existence of an alternative in-frame start codon that would lead to an N-terminal extension by a HTH-domain, followed by a coiled-coil region (Figure 4C). This observation was also noted by Rostock and colleagues[26] and implies that the original annotation of the AlbA gene is incomplete. Analogously to TipA, two versions of AlbA may exist in cells: AlbA-L, capable of driving transcriptional events after binding to albicidin and AlbA-S/AlbA$_{wt}$, which removes free albicidin from cells (Figure 4C). In the TipA system, the S version is expressed at a > 20-fold excess when compared to the L version, presumably because far fewer DNA-binding protein copies (TipA-L) are required than those simply neutralizing the thiopeptide antibiotics (TipA-S)[17]. Interestingly, in the work describing the discovery of AlbA, it was noted that the minimal DNA fragment providing albicidin resistance contained two gene products, which appeared to be under the control of one promotor[18]. They were believed to be two different proteins, but their relative abundance roughly reflected the 1 : 20 ratio observed for TipA-L and TipA-S and their molecular weights are in agreement with the predicted molecular weight of AlbA-L and the observed molecular weight of AlbA-S[18]. If this hypothesis were correct, exposure of *albA*-positive bacteria to albicidin would be expected to induce transcription of AlbA. We thus treated *albA*-positive *K. pneumoniae*, which are fully resistant to albicidin and harbor the M131Q mutation, with albicidin and analyzed the transcription levels of AlbA-L and AlbA-S by RT-qPCR at different time-points (Figure 4D). 10 min after exposure, virtually no change in AlbA transcription levels was detected, while transcription was upregulated ~ 60-fold 90 min after the addition of albicidin. After 4 h, transcription levels were upregulated ~3000-fold, indicating a very strong response to albicidin. These data suggest that AlbA acts in a manner similar to TipA, where binding of the effector molecule triggers protein expression of the effector-binding protein.

Since TipA is able to bind structurally diverse thiopeptides, we wondered if AlbA$_{wt}$ is also able to bind other compounds, in particular cystobactamid. The K_D of AlbA$_{wt}$ for an albicidin derivative with cystobactamid-like features (**5**, Figure S24) was reported as 14 nM based on a fluorescene quenching assay[26]. Yet despite this tight interaction, the antibacterial effects of **5** were not neutralized by AlbA in agar diffusion assays and **5** did not stabilize AlbA in NMR experiments[26]. SPR experiments using **7** and AlbA$_{wt}$ suggest a K_D in the low µM range (Figure S25), which may reconcile affinity with NMR data and agar diffusion assay results. To probe the effect of AlbA$_{wt}$ on **7**, we incubated it with protein to investigate if AlbA$_{wt}$, AlbA^{T99V}, AlbA^{M131A} or AlbA^{M131Q} were able to also promote the cyclization of cystobactamid (convert the central β-methoxy-asparagine into an aspartimide). Even after extensive incubation times at 37 °C, we did not observe any modification of cystobactamid (Figure S25). When comparing the MICs of **1** and **7** for *E.coli* BL21 and *E.coli* BL21 overexpressing AlbA$_{wt}$, we found no difference, perhaps because the cells were extremely sensitive to both compounds (Figure 4A). The M131K mutant also provided protection against **7,** but not to the same extent as against **1** (Figure 4A). Since *albA*-containing *K. pneumoniae* have an MIC against both compounds of > 64 µg mL^{-1}, we investigated bacterial growth after addition of either **1** or **7**

. While cultures continued to grow, only **7**, but not **1**, had a statistically significant negative effect on bacterial growth (Figure S25). Finally, we tested whether **7** was also able to induce an increase in AlbA copy numbers in *K. pneumoniae* by RT-qPCR. In striking contrast to **1**, cystobactamid 919-2 was unable to increase *albA* RNA copy numbers, even 4 h after the addition of compound (Figure 4D). These data hint that binding of **7** is insufficient to cause the dimerization of AlbA-L and thus drive transcription of the *albA* gene. We modelled the interaction of **7** and $AlbA_{wt}$ to rationalize the differences in binding between the two compounds (Figure S24). Which AlbA-independent resistance mechanism is employed by *K. pneumoniae* to protect against cystobactamid will require further study.

The internal gene duplication of the TipA-S-like antibiotic binding domain changes the architecture of the protein to allow binding of extended, hydrophobic antibiotics in a binding tunnel. This raises the question how wide-spread this new architecture actually is. When we analyzed all > 3000 UniProt sequences listed in Pfam as containing TipA, we found that the duplication of the TipA-S region has occurred exactly twice in the evolution of this family (Figure S26). One branch contains AlbA and related sequences, which are a colorful mixture of beta- and gamma-proteobacteria and enterobacteria. Overall, this branch contains an assortment of TipA sequences with and without the internal gene duplication. Curiously, the second branch is very compact and contains exclusively TipA-like proteins with a duplication of TipA-S. All of these sequences are from *Clostridiae*, including *C. botulinum*, and part of a larger *Clostridium* branch (Figure S26). They belong to the larger family of MerR-type transcriptional regulators and also encode an N-terminal HTH domain, followed by a coiled-coil region, reflecting the TipA and AlbA architecture. It is completely unclear which extended, hydrophobic natural product is bound by the proteins belonging to the second branch, or which transcriptional events are triggered in *Clostridiae* upon exposure.

Discussion

The vast majority of currently used antibiotics have been isolated from microorganisms and modified for clinical application. From an evolutionary standpoint it is intuitive to search in this space – microbes have evolved to secure and defend their ecological niche from other microbes, often using antibiotics as chemical weapons. But this also poses an inherent problem: if an antibiotic has been used for eons, it is only logical that defense strategies – antibiotic resistance – have also evolved. These resistance mechanisms then preexist in the microbial population and can be disseminated if a particular antibiotic finds broad use, for example in human antibiotic therapy. To circumvent this problem, rational compound design is required, which relies on a detailed understanding of these mechanisms of resistance. In determining the structure of AlbA, we sought to enable the design of compounds circumventing AlbA-mediated resistance. Unexpectedly, the structure revealed AlbA to be a member of the TipA family of multi-drug resistance autoregulatory systems. Consequently, the AlbA gene was reevaluated and an alternative upstream start codon found, which may give rise to AlbA-L and AlbA-S analogously to TipA. What transcriptional events may be controlled by AlbA-L will require further study. It is unclear if AlbA itself is a multi-drug resistance protein or merely evolved from such a system, since the AlbA system is not induced by the related cystobactamid. However, the observation that the internal gene duplication of the effector binding site leads to a complete change in binding-site architecture and provides a new antibiotic binding scaffold highlights the adaptability of antibiotic resistance mechanisms.

TipA is able to form a covalent complex with diverse thiopeptide antibiotics, which sequesters them from the cytoplasm and thus inactivates them. AlbA is unable to form a covalent bond with albicidin, but forms an exceptionally stable complex[31] from which albicidin dissociates very slowly. In addition, we discovered that AlbA promotes the cyclization of albicidin, which leads to a loss of activity and decreased affinity. The mechanism of very tight binding combined with slow chemical modification may also be beneficial for transcriptional control, since it allows elevated transcription to cede once exposure to albicidin is stopped. In AlbA, the combination of high-affinity binding with chemical modification may be a way to approximate the beneficial effect of the covalent TipA-thiopeptide bond. It also opens the possibility of acquired AlbA mutations, which lead to faster cyclization of albicidin and in turn a lower energetic burden on cells, since only sub-stoichiometric quantities of AlbA-S would then be required. A first step in that direction may be the M131K mutation observed in *K. pneumoniae*. This underscores the importance of investigating resistance mechanisms in detail to accelerate the developments of new antibiotics circumventing preexisting resistance mechanisms.

ASSOCIATED CONTENT

Supporting Information

The Supporting Information is available free of charge on the ACS Publications website.

Materials and Methods, supplementary figures and the table for crystallographic data can be found in the SOI PDF file. A vector map of the phylogenetic tree has been uploaded separately.

AUTHOR INFORMATION

Corresponding Author

* jesko.koehnke@helmholtz-hzi.de

Funding Sources

J.K. acknowledges the DFG for an Emmy-Noether Fellowship (KO 4116/3-1).

ACKNOWLEDGMENT

We thank Daniel Sauer for the help he provided with mass spectrometry and Prof. Lawrence Shapiro for critical reading of the manuscript. The authors are grateful for access to ESRF beamlines ID29 and ID23-1.

REFERENCES

(1) Cragg, G. M.; Newman, D. J., Natural Products: A Continuing Source of Novel Drug Leads. *Biochim Biophys Acta* **2013,** *1830*, 3670-95.

(2) Dias, D. A.; Urban, S.; Roessner, U., A Historical Overview of Natural Products in Drug Discovery. *Metabolites* **2012,** *2*, 303-36.

(3) Ventola, C. L., The Antibiotic Resistance Crisis: Part 1: Causes and Threats. *P T* **2015,** *40*, 277-83.

(4) Fair, R. J.; Tor, Y., Antibiotics and Bacterial Resistance in the 21st Century. *Perspect Medicin Chem* **2014,** *6*, 25-64.

(5) Exner, M.; Bhattacharya, S.; Christiansen, B.; Gebel, J.; Goroncy-Bermes, P.; Hartemann, P.; Heeg, P.; Ilschner, C.; Kramer, A.; Larson, E.; Merkens, W.; Mielke, M.; Oltmanns, P.; Ross, B.; Rotter, M.; Schmithausen, R. M.; Sonntag, H. G.; Trautmann, M., Antibiotic Resistance: What is so Special about Multidrug-Resistant Gram-Negative Bacteria? *GMS Hyg Infect Control* **2017,** *12*, Doc05.

(6) Nikaido, H., Multidrug Resistance in Bacteria. *Annu Rev Biochem* **2009,** *78*, 119-46.

(7) Dever, L. A.; Dermody, T. S., Mechanisms of Bacterial Resistance to Antibiotics. *Arch Intern Med* **1991,** *151*, 886-95.

(8) Munita, J. M.; Arias, C. A., Mechanisms of Antibiotic Resistance. *Microbiol Spectr* **2016,** *4*.

(9) Goh, E. B.; Yim, G.; Tsui, W.; McClure, J.; Surette, M. G.; Davies, J., Transcriptional Modulation of Bacterial Gene Expression by Subinhibitory Concentrations of Antibiotics. *Proc Natl Acad Sci U S A* **2002,** *99*, 17025-30.

(10) Davies, J.; Spiegelman, G. B.; Yim, G., The World of Subinhibitory Antibiotic Concentrations. *Curr Opin Microbiol* **2006,** *9*, 445-53.

(11) Murakami, T.; Holt, T. G.; Thompson, C. J., Thiostrepton-Induced Gene Expression in Streptomyces Lividans. *J Bacteriol* **1989,** *171*, 1459-66.

(12) Chiu, M. L.; Folcher, M.; Griffin, P.; Holt, T.; Klatt, T.; Thompson, C. J., Characterization of the Covalent Binding of Thiostrepton to a Thiostrepton-Induced Protein from Streptomyces Lividans. *Biochemistry* **1996,** *35*, 2332-41.

(13) Summers, A. O., Untwist and Shout: A Heavy Metal-Responsive Transcriptional Regulator. *J Bacteriol* **1992,** *174*, 3097-101.

(14) Barrineau, P.; Gilbert, P.; Jackson, W. J.; Jones, C. S.; Summers, A. O.; Wisdom, S., The DNA Sequence of the Mercury Resistance Operon of the Incfii Plasmid Nr1. *J Mol Appl Genet* **1984,** *2*, 601-19.

(15) Kahmann, J. D.; Sass, H. J.; Allan, M. G.; Seto, H.; Thompson, C. J.; Grzesiek, S., Structural Basis for Antibiotic Recognition by the Tipa Class of Multidrug-Resistance Transcriptional Regulators. *EMBO J* **2003,** *22*, 1824-34.

(16) Habazettl, J.; Allan, M.; Jensen, P. R.; Sass, H. J.; Thompson, C. J.; Grzesiek, S., Structural Basis and Dynamics of Multidrug Recognition in a Minimal Bacterial Multidrug Resistance System. *Proc Natl Acad Sci U S A* **2014,** *111*, E5498-507.

(17) Holmes, D. J.; Caso, J. L.; Thompson, C. J., Autogenous Transcriptional Activation of a Thiostrepton-Induced Gene in Streptomyces Lividans. *EMBO J* **1993,** *12*, 3183-91.

(18) Walker, M. J.; Birch, R. G.; Pemberton, J. M., Cloning and Characterization of an Albicidin Resistance Gene from Klebsiella Oxytoca. *Mol Microbiol* **1988,** *2*, 443-54.

(19) Chiu, M. L.; Viollier, P. H.; Katoh, T.; Ramsden, J. J.; Thompson, C. J., Ligand-Induced Changes in the Streptomyces Lividans Tipal Protein Imply an Alternative Mechanism of Transcriptional Activation for Merr-Like Proteins. *Biochemistry* **2001,** *40*, 12950-8.

(20) Kretz, J.; Kerwat, D.; Schubert, V.; Gratz, S.; Pesic, A.; Semsary, S.; Cociancich, S.; Royer, M.; Sussmuth, R. D., Total Synthesis of Albicidin: A Lead Structure from Xanthomonas Albilineans for Potent Antibacterial Gyrase Inhibitors. *Angew Chem Int Ed Engl* **2015,** *54*, 1969-73.

(21) Baumann, S.; Herrmann, J.; Raju, R.; Steinmetz, H.; Mohr, K. I.; Huttel, S.; Harmrolfs, K.; Stadler, M.; Muller, R., Cystobactamids: Myxobacterial Topoisomerase Inhibitors Exhibiting Potent Antibacterial Activity. *Angew Chem Int Ed Engl* **2014,** *53*, 14605-9.

(22) Birch, R. G.; Patil, S. S., Preliminary Characterization of an Antibiotic Produced by Xanthomonas Albilineans which Inhibits DNA Synthesis in Escherichia Coli. *J Gen Microbiol* **1985,** *131*, 1069-75.

(23) Birch, R. G., Xanthomonas Albilineans and the Antipathogenesis Approach to Disease Control. *Mol Plant Pathol* **2001,** *2*, 1-11.

(24) Rott, P. C.; Costet, L.; Davis, M. J.; Frutos, R.; Gabriel, D. W., At least two Separate Gene Clusters are Involved in Albicidin Production by Xanthomonas Albilineans. *J Bacteriol* **1996,** *178*, 4590-6.

(25) Hashimi, S. M.; Wall, M. K.; Smith, A. B.; Maxwell, A.; Birch, R. G., The Phytotoxin Albicidin is a Novel Inhibitor of DNA Gyrase. *Antimicrob Agents Chemother* **2007,** *51*, 181-7.

(26) Rostock, L.; Driller, R.; Gratz, S.; Kerwat, D.; von Eckardstein, L.; Petras, D.; Kunert, M.; Alings, C.; Schmitt, F. J.; Friedrich, T.; Wahl, M. C.; Loll, B.; Mainz, A.; Sussmuth, R. D., Molecular Insights into Antibiotic Resistance - How a Binding Protein Traps Albicidin. *Nat Commun* **2018,** *9*, 3095.

(27) Basnayake, W. V.; Birch, R. G., A Gene from Alcaligenes Denitrificans that Confers Albicidin Resistance by Reversible Antibiotic Binding. *Microbiology* **1995,** *141 (Pt 3)*, 551-60.

(28) Zhang, L.; Birch, R. G., The Gene for Albicidin Detoxification from Pantoea Dispersa Encodes an Esterase and Attenuates Pathogenicity of Xanthomonas Albilineans to Sugarcane. *Proc Natl Acad Sci U S A* **1997,** *94*, 9984-9.

(29) Weng, L. X.; Wang, L. H.; Xu, J. L.; Wu, J. E.; Li, Q.; Zhang, L. H., Molecular and Conformational Basis of a Specific and High-Affinity Interaction between Alba and Albicidin Phytotoxin. *Appl Environ Microbiol* **2005,** *71*, 1445-52.

(30) Weng, L. X.; Xu, J. L.; Li, Q.; Birch, R. G.; Zhang, L. H., Identification of the Essential Histidine Residue for High-Affinity Binding of Alba Protein to Albicidin Antibiotics. *Microbiology* **2003,** *149*, 451-7.

(31) Zhang, L.; Xu, J.; Birch, R. G., High Affinity Binding of Albicidin Phytotoxins by the Alba Protein from Klebsiella Oxytoca. *Microbiology* **1998,** *144 (Pt 2)*, 555-9.

(32) Holm, L.; Rosenstrom, P., Dali Server: Conservation Mapping in 3d. *Nucleic Acids Res* **2010,** *38*, W545-9.

(33) Chiu, M. L.; Folcher, M.; Katoh, T.; Puglia, A. M.; Vohradsky, J.; Yun, B. S.; Seto, H.; Thompson, C. J., Broad Spectrum Thiopeptide Recognition Specificity of the Streptomyces Lividans Tipal Protein and its Role in Regulating Gene Expression. *J Biol Chem* **1999,** *274*, 20578-86.

(34) Gratz, S.; Kerwat, D.; Kretz, J.; von Eckardstein, L.; Semsary, S.; Seidel, M.; Kunert, M.; Weston, J. B.; Sussmuth, R. D., Synthesis and Antimicrobial Activity of Albicidin Derivatives with Variations of the Central Cyanoalanine Building Block. *ChemMedChem* **2016,** *11*, 1499-502.

The structure of AlbA reveals it to be a new binding scaffold adapted to the sequestration of long-chain antibiotics and a member of the multi-antibiotic neutralizing TipA family. Unexpectedly, AlbA promoted the chemical modification of albicidin, which reduced albicidin potency.